31st Annual International Conference of the IEEE EMBS
Minneapolis, Minnesota, USA, September 2-6, 2009

Pulse-Clamp Technique for Single Neuron Stimulation Electrode Characterization

André van Ooyen, Volker G. Zagolla, Christian Ulrich, Uwe Schnakenberg

Abstract— **Miniaturized electrodes, structures and devices are necessary to achieve high target selectivity during stimulation in single neuron networks, while significant charge transfer is still demanded. A reliable test method is required to evaluate charge injection capability for high resolution neural stimulation applications that demand both a large amount of charge injection and a small electrode size. A circuit designed for the pulse-clamp technique was employed to characterize the electrode charge-storage capability of microelectrodes of sizes smaller than 300 μm in diameter. The circuit allows different electrodes and surface modifications to be quickly and accurately compared. Pulse-clamp measurements are performed on planar microelectrodes in 154 mM phosphate buffered saline (PBS) solution with 400 μs long pulses at charges up to 40 nC. The pulse-clamp and cyclic voltammetry results of sputtered iridium oxide film (SIROF) electrodes of different sizes show charge losses of less than 3% and a superior reversible charge injection capability compared to platinum microelectrodes of the same size, even at higher charge density levels.**

I. Introduction

The design of novel bidirectional interfaces for in vitro single neuron networks is an important step towards the use and understanding of neuronal coupling to electronics and neuronal enhanced signal processing in biohybrid circuits. Current and future neural prostheses are based on electrical stimulation of neurons, which help to restore functionality to patients suffering from neurodegenerative diseases. Such devices typically feature electrodes based on either platinum, titanium nitride, or iridium oxide (IrOx). A number of reports, documenting the use of IrOx microelectrodes for neuroengineering and biomedical applications, have been presented ([1], [2], [3], [4]). The interest in this material is driven by its excellent properties as a functional coating for implantable stimulation electrodes, as it retains a high and reversible charge capture and delivery capacity. Since the traditional electrochemical tests, i.e. cyclic voltammetry (CV) and impedance analysis, do not operate at the same time scale or voltage amplitudes as is required in neural stimulation, they are inadequate to investigate the true electrode dynamics. Therefore a reliable test method is needed to evaluate the charge injection capability at the neuron/electrode interface, since high resolution neural stimulation demands both a large amount of charge injection and a small electrode size. These requirements are met by the pulse-clamp technique, first developed and introduced by Mortimer and co-workers [8] and also used by Hung et al. [9]. An improved custom circuit was designed and is currently used to characterize the electrode charge-injection capability of planar disc microelectrodes with a functional layer of sputtered iridium oxide film (SIROF) ([5], [6], [7]) The focus of this paper is to examine and discuss the use of the pulse-clamp technique to characterize single neuron stimulation electrodes. We report preliminary results of pulse-clamping experiments on SIROF electrodes with diameters smaller than 300 μm.

This work was supported by the German Research Foundation Agency under grant No. SCHN 587/5-1 "Mi-Besan"

All authors are with the Institute of Materials in Electrical Engineering I, RWTH Aachen University, 52074 Aachen, Germany (email: vanooyen@iwe1.rwth-aachen.de)

II. Materials & Methods

Microelectrode arrays (MEAs) were fabricated through a custom technological process. Briefly, a reversal photoresist lift-off technique (AZ nLof 2035, Clariant, Germany) was employed to pattern gold metal on a silicon substrate. The iridium oxide layer was sputter-deposited as described in [7] using a Nordiko NS2550 sputtering tool, with the following parameters: 180W DC power, 100 sccm argon flow and 10.4 sccm oxygen flow. A layer of parylene-C (3 μm) was used as an insulating layer, covering the leads while leaving free access to the electrodes sites and contacts.

The MEA layout consisted of a 4×4 square grid arrangement of 16 circular microelectrodes with exposed areas measuring 25, 50, 100, and 300 μm in diameter (Fig. 1). MEAs were glued onto printed circuit boards (PCB) to provide external interfacing to the pulse-clamping electronics. Platinum-based MEAs, with identical layout and electrode geometry, were also fabricated and employed for comparison. Finally, a glass ring (diameter 20 mm), glued to the PCB base plate with epoxy (EpoTek OG301, Polytec), formed a chamber with a volume of 1.5 ml.

The principle of the pulse-clamp technique is to perform

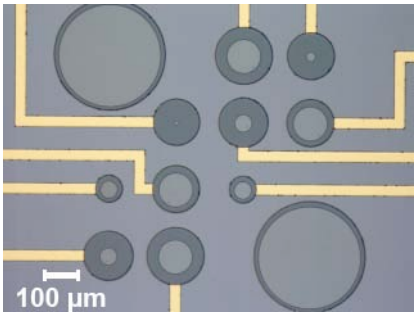

Fig. 1: Photolithographically fabricated SIROF microelectrode array showing the different electrode sizes.

a discharge current measurement with a high time resolution after an electrode has been charged by a current pulse. First the working electrode is set to a potential, e.g. 0 V, versus the reference electrode. During testing, the instrument switches to current mode and forces a constant-current (cathodic or anodic), simulating half of the neural-stimulation pulse sequence, called the current clamp (CC).

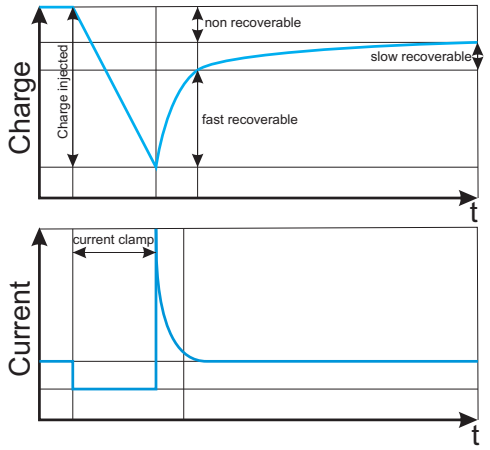

Fig. 2: Current and charge behavior during a pulse-clamp experiment.

Directly after this current pulse the potential of the stimulation electrode is fixed to the same value as before the pulse, instead of immediately following with a second current pulse of equal charge and opposite polarity. This stage is called the potential clamp (PC).

By integration of the measured current during PC it is possible to calculate the charge regained. As can be seen in Fig. 2, a certain amount of charge is injected during the CC, followed by a discharging phase during the PC. Three different stages in the discharge phase can be identified: the fast discharge directly after the CC, correlated to fast recoverable electrochemical processes, the slow discharge, based on slow recoverable processes and a certain difference of charge which cannot be recovered due to being stored in permanent products of faradaic processes. If the electrode behaves as a pure resistor, no stored charge will be recovered. Conversely, if the electrode behaves as an ideal capacitor, all of the injected charge will be recovered. To characterize the SIROF microelectrodes a pulse-clamp circuit was designed, which operates similar to the setup used earlier by Mortimer and co-workers [8]. To evaluate electrodes of a size below 300 µm the existing circuit had to be improved to be able to facilitate a very high switching speed between the constant-current charging mode and the constant-voltage discharging mode. These improvements resulted in a pulse-clamp circuit that reached an overall switching time of <1 µs, including slew rate and settling time. Our circuit remains stable during high speed operation at low current values and achieves a lowest current resolution of 100 nA/V. The circuit function was verified by using a standard Randles cell model [10] that is extended to a model shown in Fig. 3 as a device under test.

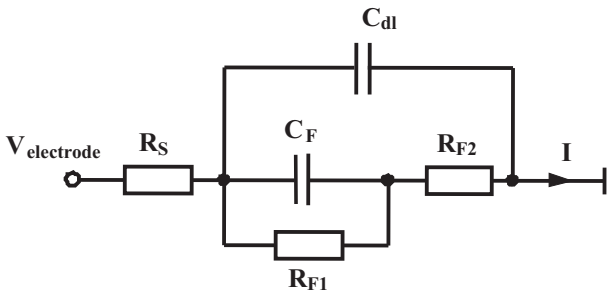

Fig. 3: Model of the electrode/electrolyte interface based on the Randles cell model.

The extended cell adds an impedance consisting of C_F, R_{F1} and R_{F2} to the Randles cell model. This models the behavior of the slow (C_F) and non recoverable processes (R_{F1}). The resistance R_{F2} defines the charge and discharge rates of C_F. Additionally the measured results from the dummy cell where compared with SPICE simulations (data not shown). During the pulse-clamp most of the injected charge is stored in the two capacitances and discharged through both the solution (R_S) and faradaic charge resistances (R_{F1},R_{F2}).

III. Experimental

All experiments were conducted on planar SIROF microelectrodes featuring a film thickness of 300 nm, with a circular opening in the parylene-C insulation. Phosphate buffered saline (PBS) solution with 154 mM NaCl was used as the electrolyte in all experiments. The setup used consists of the improved pulse-clamp circuit and a National Instruments NI USB-6125 device for data acquisition at a sample rate of 1.25 MS/s and a resolution of 16 bits, which complies with demands set by the pulse-clamp circuit regarding speed and resolution. Using a custom designed LabVIEW program the current is measured and the corresponding charge is obtained by calculating the time integral. To ensure that no water electrolysis or electrode dissolution occured all experiments where performed within the charge injection limits [11] given in Tab. I. To characterize the microelectrodes two different experiments were conducted; cyclic voltammetry and pulse-clamping.The CV was conducted to identify the electrochemical reactions as well as their reversibility. For the comparison of the SIROF and platinum electrodes the cathodal charge storage capacity (CSC_c) was calculated by

TABLE I: Charge injection limits and potential limits.

Material	Charge Injection Limit (mC/cm^2)	Potential Limits (V vs. Ag/AgCl)
Platinum	0.05 - 0.15	-0.6 - 0.8
SIROF	1 - 5	-0.6 - 0.8

integration of the cathodal current of a slow-sweep-rate CV, within a potential range inside the water electrolysis window, namely -0.6 V to 0.8 V vs. Ag/AgCl.

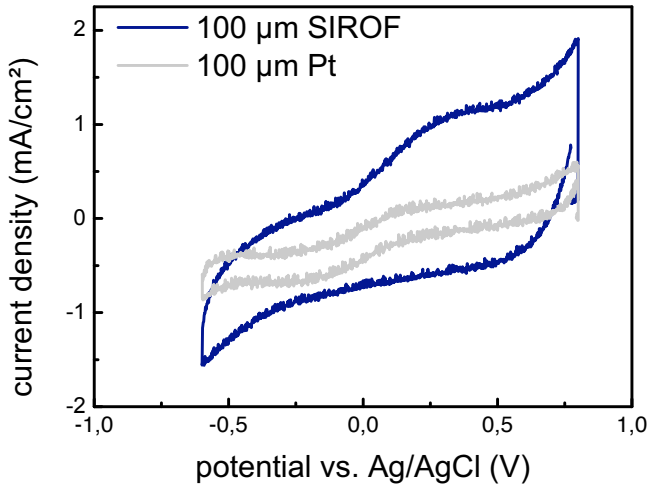

Fig. 4: Cyclic voltammograms of SIROF and Pt electrodes of 100 µm in diameter.

IV. Results & Discussion

Fig. 4 shows CV measurements of SIROF and platinum between -0.6 V and 0.8 V vs Ag/AgCl at a scan rate of 50 mV/s. Due to its fractal surface morphology, the SIROF's capacity for storing charge is significantly higher compared to platinum, which is reflected in its CV. The higher charge injection capabilities of SIROF also result from a reversible faradaic reaction which involves reduction and oxidation between the Ir^{3+} and Ir^{4+} states of the oxide [12]. The resulting CSC_cs of the voltammograms are 16.7 mC/cm^2 and 5.7 mC/cm^2 for SIROF and platinum, respectively.

Fig. 5 illustrates the current and the corresponding charge of two SIROF microelectrodes, one having a 100 µm diameter (approx. 7850 µm^2) and the other 25 µm (approx. 500 µm^2), during a pulse-clamp experiment. The current pulse width was kept constant at 400 µs and the magnitude of the current during the CC was adjusted to be safely within the charge injection limits given in Tab. I. The amount of charge recovered in this process is higher than 97% for both electrodes as shown in Tab. II. Comparing the discharge stages of the two electrodes, it can be observed that the 100 µm electrode has a slower discharge compared to the 25 µm one. Most likely due to different capacitances and therefore different RC time constants. Despite this the ratio of the lost charge compared to the injected charge is nearly the same after t = 20 ms. During the discharge phase the charge stored capacitively, such as in the double-layer, is returned rapidly (fast reversible) followed by the slower processes, involving the Ir^{3+}/Ir^{4+} redox couple (eq. 1).

$$Ir^{3+} \leftrightarrow Ir^{4+} + e^- \quad (1)$$

This faradaic reaction is confined to the SIROF layer and appears to be a almost reversible process. The faradaic process of water electrolysis is avoided in the experiments done by not exceeding the -0.6 V/0.8 V potential window. The actual charge loss measured might result from faradaic reactions involving trace impurities in the IrOx film.

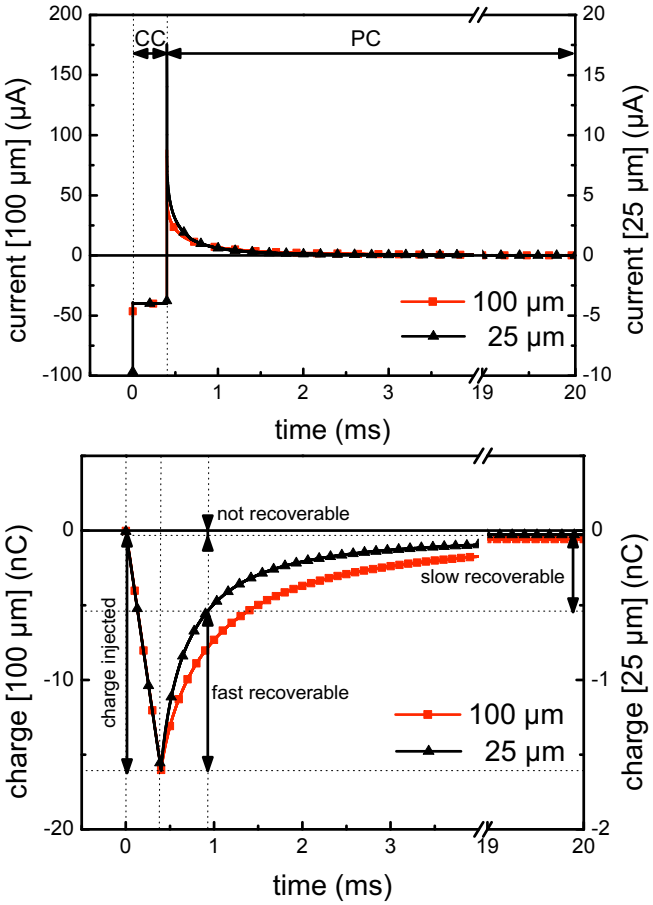

Fig. 5: Measured current of SIROF microelectrodes with different sizes while applying a 400 µs long pulse and its correlated charge retrieved by integration over time.

TABLE II: Charge injected, discharge and charge lost for the two electrodes in Fig. 5.

Electrode	Charge injected (nC)	Discharge (nC)	Charge lost (nC) / (%)
100µm	23.93	-23.35	0.58 / 2.42%
25µm	2.39	-2.331	0.059 / 2.47%

In Fig. 6 an example of a pulse-clamp analysis is given, illustrating the charge lost vs. the charge injected into the electrochemical cell during the CC while gradually increasing the absolute applied current. As can be seen, there exists a near linear correlation between the charge injected and the charge lost, for both SIROF electrode sizes. The difference between the 25 µm electrode values compared to the 100 µm electrode most likely results from the circuit inherent noise and consequently its smaller SNR.

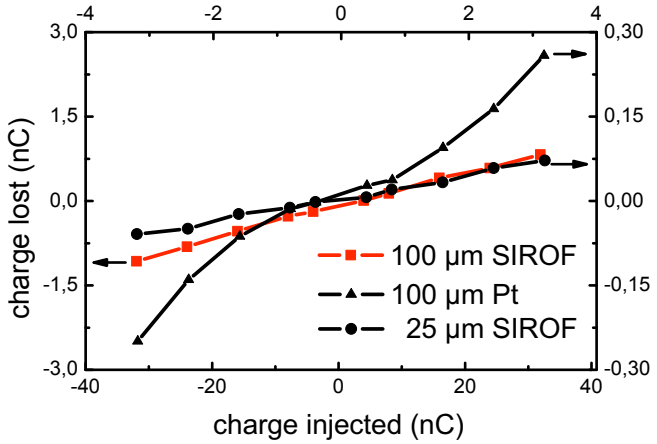

Fig. 6: Charge lost vs. charge injected for two SIROF microelectrodes and a Pt electrode. During the experiments the charge density was kept at approximatly the same level.

Also shown in Fig. 6 is an analysis of a 100 µm platinum microelectrode using the same scale as the 25 µm SIROF electrode. For small charge injections the platinum electrode displays a similar behavior as the SIROF electrodes but when the absolute value of charge injection is increased beyond 1 nC the amount of charge lost increases significantly. This can be related to a lower double layer capacitance and limited redox reactions of the Pt metal. The data indicate that SIROF can inject high amounts of charge over a broad range keeping the same charge lost/injected ratio compared to platinum electrodes of the same geometrical area. This higher charge injection capability of SIROF is based on its surface morphology and to some part on the fast and reversible Ir^{3+}/Ir^{4+} redox reaction mentioned above.

V. Conclusion

This work demonstrates the use of the pulse-clamp technique as both a fast and accurate method for characterizing the charge-injection capabilities of SIROF microelectrodes. The scalability of the pulse-clamp technique allows it to be used to accurately quantify the quality of a surface modification for microelectrodes well below 300 µm in diameter. By applying the pulse-clamp technique it can be seen that when very low charge densities are applied nearly no charge loss is present due to the double-layer capacitance charge storage or reversible Ir^{3+}/Ir^{4+} redox reactions. However, the charge loss cannot be totally avoided as has been shown before by Brummer and co-workers [13]. The pulse-clamp results of SIROF electrodes of different sizes show charge losses less than 3% and a superior reversible charge injection capability compared to platinum microelectrodes of the same size, even at higher charge density levels. The pulse-clamp technique allows an accurate electrode parameter extraction and a comparison of the charge-injection capabilities of different electrode sizes and materials. To maintain stability of the circuit when measuring smaller electrodes down to 10 µm and below, compensation capacitances have to be increased which slow down the switching speed due to higher RC constants. This affects the achievable resolution for the fast discharge current components which has to be considered when the electrode size is decreased. In ongoing investigations the pulse-clamp technique is applied to smaller electrodes sizes down to 10 µm to quantify charge-injection limits for single neuron stimulation applications.

VI. Acknowledgments

This work was supported by by the German Research Foundation Agency under grant No. SCHN 587/5-1 "Mi-Besan".

References

[1] A. Blau, C. Ziegler, M. Heyer, F. Endres, G. Schwitzgebel, T. Matthies, T. Stieglitz, J. U. Meyer, and W. Gopel, "Characterization and optimization of microelectrode arrays for in vivo nerve signal recording and stimulation," *Biosensors & Bioelectronics*, vol. 12, no. 9-10, pp. 883–892, 1997.

[2] S. F. Cogan, "In vivo and in vitro differences in the charge-injection and electrochemical properties of iridium oxide electrodes," *Engineering in Medicine and Biology Society, 2006. EMBS '06. 28th Annual International Conference of the IEEE*, pp. 882 – 885, Jan 2006.

[3] S. Marzouk, S. Ufer, R. Buck, T. Johnson, L. Dunlap, and W. Cascio, "Electrodeposited iridium oxide ph electrode for measurement of extracellular myocardial acidosis during acute ischemia," *Analytical Chemistry*, vol. 70, no. 23, pp. 5054–5061, DEC 1 1998.

[4] W. Mokwa, *Comprehensive Microsystems*. Oxford, Elsevier Science, 2007, vol. 3, ch. Artificial retinas, pp. 201–217.

[5] E. Slavcheva, R. Vitushinsky, W. Mokwa, and U. Schnakenberg, "Sputtered iridium oxide films as charge injection material for functional electrostimulation," *Journal of the Electrochemical Society*, vol. 151, no. 7, pp. E226–E237, 2004.

[6] A. van Ooyen, B. Wessling, E. Slavcheva, and U. Schnakenberg, "Evaluation of sirof microelectrodes for single neuron stimulation in biohybrid circuits," *International Solid-State Sensors, Actuators and Microsystems Conference, 2007. TRANSDUCERS 2007.*, pp. 1227 – 1230, May 2007.

[7] B. Wessling, W. Mokwa, and U. Schnakenberg, "Sputtered ir films evaluated for electrochemical performance - i. experimental results," *Journal of the Electrochemical Society*, vol. 155, no. 5, pp. F61–F65, 2008.

[8] M. Bonner, M. Daroux, T. Crish, and J. Mortimer, "The pulse-clamp method for analyzing the electrochemistry on neural stimulating electrodes," *Journal of the Electrochemical Society*, vol. 140, no. 10, pp. 2740–2744, OCT 1993.

[9] A. Hung, D. Zhou, R. Greenberg, I. B. Goldberg, and J. W. Judy, "Pulse-clamp technique for characterizing neural-stimulating electrodes," *Journal of the Electrochemical Society*, vol. 154, no. 9, pp. C479–C486, 2007.

[10] J. E. B. Randles, "Kinetics of rapid electrode reactions," *Discussions of the Faraday Society*, vol. 1, pp. 11–19, 1947.

[11] T. L. Rose and L. S. Robblee, "Electrical stimulation with pt electrodes: 8. electrochemically safe charge injection limits with 0.2 ms pulses," *IEEE Trans. Biomed. Eng.*, vol. 37, no. 11, pp. 1118–1120, NOV 1990.

[12] J. Mozota and B. E. Conway, "Surface and bulk processes at oxidized iridium electrodes .1. monolayer stage and transition to reversible multilayer oxide film behavior," *Electrochimica Acta*, vol. 28, no. 1, pp. 1–8, 1983.

[13] J. McHardy, L. S. Robblee, J. M. Marston, and S. B. Brummer, "Electrical stimulation with pt electrodes: 4. factors influencing pt dissolution in inorganic saline," *Biomaterials*, vol. 1, no. 3, pp. 129–134, 1980.